PUNCTURE PERFORMANCE OF THE CAUDAL SPINES FROM TWO COASTAL STINGRAYS, *HYPANUS SAY* AND *HYPANUS SABINUS*

by

Caitlin Shea-Vantine

A Thesis Submitted to the Faculty of

The Charles E. Schmidt College of Science

In Partial Fulfillment of the Requirements for the Degree of

Master of Science

Florida Atlantic University

Boca Raton, FL

May 2020

PUNCTURE PERFORMANCE OF THE CADUAL SPINES OF TWO COASTAL STINGRAYS, *HYPANUS SAY* AND *HYPANUS SABINUS*

by

Caitlin Shea-Vantine

This thesis was prepared under the direction of the candidate's thesis advisor, Dr. Stephen Kajiura, Department of Biological Sciences, and has been approved by all members of the supervisory committee. It was submitted to the faculty of the Charles E. Schmidt College of Science and was accepted in partial fulfillment of the requirements for the degree of Master of Science.

SUPERVISORY COMMITTEE:

Stephen Kajiura
Stephen Kajiura (May 7, 2020)

Stephen M. Kajiura, Ph.D.
Thesis Advisor

Marianne E. Porter, Ph.D.

Tricia L. Meredith, Ph.D.

SL Milton
Sarah Milton (May 8, 2020)

Sarah L Milton, Ph.D.
Chair, Department of Biological Sciences

Ata Sarajedini, Ph.D.
Dean, Charles E. Schmidt College of Science

Robert W. Stackman Jr., Ph.D.
Dean, Graduate College

May 8th, 2020
Date

ACKNOWLEDGEMENTS

Funding for this project was provided by the Palm Beach County Fishing Foundation through the Capt. Al Nathan Memorial Scholarship. I would like to thank Dr. C. Bedore and M. McCallister for helping me acquire stingray spines. I would also like to thank K. Galloway and D. Ingle for their input and support in various stages of this project. I am grateful to the FAU Imaging Lab and FAU Biomechanics Lab for the use of their equipment as well as Kent Wallace for his technical support. I am also thankful to Dr. S Kajiura, Dr. M. Porter, and Dr. T. Meredith for their mentorship and technical assistance as well as S. Hoover and V. Garefino for discussion and reviews of this manuscript. Special thanks to L. Vantine and E. Vantine for their support during this project.

ABSTRACT

Author:	Caitlin Shea-Vantine
Title:	Puncture Performance Of The Caudal Spines From Two Coastal Stingrays, *Hypanus Say* And *Hypanus Sabinus*
Institution:	Florida Atlantic University
Thesis Advisor:	Dr. Stephen Kajiura
Degree:	Master of Science
Year:	2020

A diagnostic characteristic of stingrays in the Family Dasyatidae is the presence of a defensive, partially-serrated spine located on the tail. The objective of this study is to assess the impacts of caudal spine morphology on puncture and withdrawal performance from two stingrays, *Hypanus sabinus* and *Hypanus say*. Spines have highly variable morphology. I used an Instron E1000 materials tester to quantify the puncture and withdraw forces from porcine skin, a model for human skin. I found no significant differences between puncture and withdraw or between the species. By incorporating micro-CT scanning to quantify mineralization density, I quantified more mineralization along the shaft of the spine. Equal puncture and withdraw forces and increased mineralization along the spine shaft may create a stiffer structure that can be a persistent predator deterrent.

PUNCTURE PERFORMANCE OF THE CAUDAL SPINES FROM TWO COASTAL STINGRAYS, *HYPANUS SAY* AND *HYPANUS SABINUS*

LIST OF TABLES

LIST OF FIGURES

INTRODUCTION

In biological systems, many taxa have spines that project away from the body and interact *actively* or *passively* with the surrounding structures. In aquatic environments, sea urchin and lionfish spines are used as passive defenses against predators (Su *et al*., 2000; Galloway & Porter, 2019). Conversely, various marine organisms actively puncture using biological structures such as spurs, spines, teeth or nematocysts for defense or for prey acquisition (Huskey, 2017; Anderson *et al*., 2016; Salisbury *et al*., 2010; Perkins & Morgan, 2004; Fenner *et al*., 1996; Auerbach, 1991). Kinematics of active puncturing systems have been investigated in some marine invertebrates. For example, cone snails use a high-speed hydraulic mechanism to inject their hollow, venom-filled, spear-like radular tooth into prey. The morphology of the radular tooth aids in quick venom delivery (Salisbury *et al*., 2010). The spearing mantis shrimp, an ambush predator, use their long spear-like appendage to effectively strike prey. Spring and latch structures allow for the shrimp to produce a spring-loaded action enabling the shrimp to gain speed to strike and capture their prey (DeVries *et al*., 2012).

I gain understanding of biological projection utility by examining their mechanics, morphology, material properties, and composition. For example, North American porcupine quills are specialized hairs that have microscopic rear-facing (with respect to the quill tip) deployable barbs. These barbs will splay away from the shaft of the quill if moved in the opposite direction. This barb morphology facilitates penetration and high

tissue adhesion, which are desirable qualities for defense (Cho *et al*., 2012; Betz & Kölsch, 2004). Barbs create stress concentrations along the quill that reduce damage to the tissue by stretching muscle fibers. Barbs also catch the tissue fibers during withdrawal (Crofts & Anderson, 2018). Barb morphology and arrangement thus helps to explain the puncture force reduction required to penetrate tissue and the higher force required to withdraw from tissue.

In puncture mechanics, another morphological feature to consider is the sharpness of these biological projections. The sharpness of the tool determines which materials can be punctured. Sharpness can be captured by two parameters; included tip angle and radius of curvature (Anderson, 2018; Crofts & Anderson, 2018; Crofts *et al.,* 2019). An acute included tip angle and smaller radius of curvature result in sharper tools (Anderson et al. 2018). By investigating sharpness in conjunction with other morphological features, I can infer the biological implications of these biological projections as the animal defends itself.

Similarly to porcupines, stingrays have a defensive structure called a caudal spine (also known as a caudal barb or stinger). These serrated spines are highly modified dermal denticles that first appeared on species from the Late Cretaceous period, which also saw the rise of many large predatory sharks (Chabain *et al.,* 2019; Marmi *et al.,* 2010; Shimada, 1997; Schwimmer *et al.,* 1997). Stomach content analyses from extant species have shown that stingrays are the prey of large marine predators including, the great hammerhead shark, *Sphyrna mokarran*, (Allen, 1999; Gudger, 1946; Stevens & Lyle, 1989), tiger shark, *Galeocerdo cuvier*, (Allen, 1999; Gudger, 1946; Lowe *et al.,* 1996), bull shark, *Carcharhinus leucas*, (Cliff & Dudley, 1991; Snelson *et al.,* 1984),

goliath grouper, *Epinephelus itajara*, (NMFS, 2006; Randall, 1967) and orca whales, *Orcinus orca*, (Duignan *et al.,* 2000). Stingray spines are often broken off and found embedded in the body cavities and jaws of predators indicating their use as a defensive tool (Cliff & Dudley, 1991; Gudger, 1946; Snelson *et al.,* 1984.)

Caudal spines are comprised of mineralized collagen and are positioned on the dorsal surface of the tail. The location along the dorsal surface of the tail varies among species and the spines can be located from near the base to near the tip (Hughes *et al.,* 2018; Su *et al.,* 2017; Figure 1). In general, the caudal spine is dorso-ventrally compressed with a sharp, pointed tip, and laterally-located rear- facing serrations (with respect to the tip) on both sides (Figure 1). Previous work has investigated the possible correlation between spine morphology among freshwater and marine species (Schwartz, 2005). However, spine morphology cannot be conclusively linked to ecology or phylogenetics (Chabain, 2020, personal communication). Spine shape can be highly variable in terms of number of serrations, serrated length of spine, and spine cross-sectional shape both inter and intra-specifically (Chabain *et al.,* 2019). In addition to high morphological variation, the number of spines also varies among the species. For example, Atlantic stingrays, *Hypanus sabinus*, have a maximum of two spines at any given time and they are shed annually (Teaf & Lewis, 1987; Amesbury & Snelson, 1997). In contrast, spotted eagle rays, *Aetobatis narinari*, can have up to 8 spines (Gudger, 1914).

The spine is a two-fold defensive structure; it conveys physical insult and venom. When provoked, stingrays will elevate their tail and slash or puncture the spine into the target causing tissue damage and subsequent venom delivery (Hughes *et al.,* 2018). Vascular venomous tissue is housed within ventrolateral grooves along the length of the

spine and covered with a protective integumentary sheath, which is ruptured during puncture and allows the venom to enter the new wound (Halstead *et al.,* 1955; Russell, 1965; Enzor *et al.,* 2011; Figure 1). During the strike, the spine also embeds sandy, microbially-rich integument into the damaged tissue which remains and provides additional irritation within the wound.

The kinematics of the strike have been described in detail for only one species, the yellow stingray, *Urobatis jamaicensis* (Hughes *et al.,* 2018). This species exhibits two types of active strikes, a vertical strike and a horizontal strike. A *vertical strike* is defined as the stingray tail raising, vertically over the body and then arcing to puncture the spine into the target. A *horizontal strike* occurs as a side-to-side lashing motion, which results in a slash-like laceration (Spieler *et al.,* 2013; Hughes *et al.,* 2018). For both types of strike, a tendon traveling the length of the ventral portion of the tail will depress the tip of the tail to deploy the spine (Hughes *et al.,* 2018). The average duration of a strike is 0.23 seconds (s), and the puncture velocity is 168.14 cm s^{-1} (Hughes *et al.*, 2018). Rear-facing serrations located along the lateral sides of the spine help to puncture soft tissues, and inhibit easy removed, causing further tissue damage (Halstead & Bunker, 1953.) If the spine becomes deeply embedded into the target, it often will break off and the stingray can regrow a new one in its place (Teaf & Lewis, 1987; Amesbury & Snelson, 1997; Johansson *et al.,* 2004; Hughes *et al.,* 2018).

There a cursory understanding of the caudal spine strike kinematics, but the puncture and withdrawal forces are presently unknown. Also unexplored is the impacts of the rear-facing serrations on puncture and potential withdrawal forces. Addressing these questions will enable understanding of defense puncture mechanics of the caudal spine. This study

will assess caudal spine morphology impacts on puncture and withdrawal performance in stingrays. I test two closely related and ecologically similar species, the Bluntnose stingray, *Hypanus say* (Lesueur, 1817), and the Atlantic stingray, *Hypanus sabinus* (Lesueur, 1824). The Atlantic stingray, *H. sabinus,* is a common coastal species distributed from the Chesapeake Bay to Campeche, Mexico (Robins & Ray, 1986). It occurs in shallow, inshore coastal and estuarine habitats (Bigelow & Schroeder, 1953; Thorson, 1983; Snelson *et al.,* 1988). The Bluntnose stingray, *H. say,* has a patchy distribution in western Atlantic coastal waters from Massachusetts to southern Brazil, including the Gulf of Mexico and many islands in the Greater Antilles (Bigelow & Schroeder, 1953; Snelson *et al.,* 1989). The specific aims of this project are to: (i) describe spine morphology, (ii) quantify puncture and withdraw forces and (iii) investigate composition of the spines. I quantify caudal spine punctures forces required to penetrate and withdraw from a target material. I can correlate differences in morphology and composition and begin to define spine characteristics that contribute to the most effective and efficient puncture. Understanding the puncture and withdrawal mechanics of the caudal spine may allow us to make ecological inferences, such feasibility for reuse and effective protection.

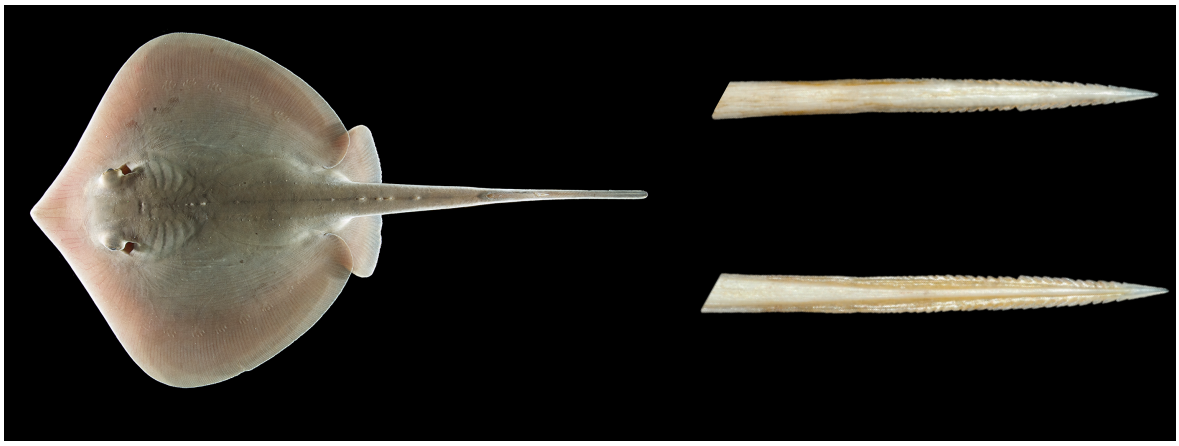

Figure 1: Hypanus sabinus (left) has a maximum of two venomous spines located approximately half way along the length of its' tail. The upper, right figure shows the dorsal view of the spine, and the lower right figure shows the ventral view of the spine.

EXPERIMENTAL METHODS

Specimen and Apparatus Preparation

Specimens of Atlantic and Bluntnose stingrays used in these experiments and they were provided by previous studies (Florida Atlantic University IACUC #A13-21, Georgia Southern University IACUC #I17001). Spines from the Bluntnose stingray (n=14) and Atlantic stingray (n=14) were dissected from the tail. In the case of specimens with two spines, *primary* spines were classified as the superior spine and the newer inferior spine as the *secondary* spine (Schwartz, 2007). Spines were cleaned with deionized water and placed on a matte background with a ruler in frame to provide scale. The spines were photographed with a Nikon D70s camera equipped with a 60mm macro lens and imported into NIH ImageJ (Schneider *et al.,* 2012). In Image J, the scale was calibrated with the ruler in frame and total spine length and total serrated length were measured. The number of serrations was also quantified from the right side of each spine (Figure 2). Serration density was calculated as serration number divided by total serrated length. Dorsal and ventral photographs of the spine tip were also taken to determine tip included angle and the radius of curvature (RoC) to quantify sharpness (Figure 3). The tip included angle was measured with the angle tool in ImageJ. The angle was described from the margins of the left and right lateral edges of the spine to the tip. The radius of curvature was determined by drawing a circle on the image of the spine tip using ImageJ. The RoC was calculated as:

$$\text{RoC} = \frac{1}{\sqrt[3]{1/R+1/R'}}$$

R (radius of the circle) denotes the dorsal view. R´ (radius of the circle) denotes the ventral view.

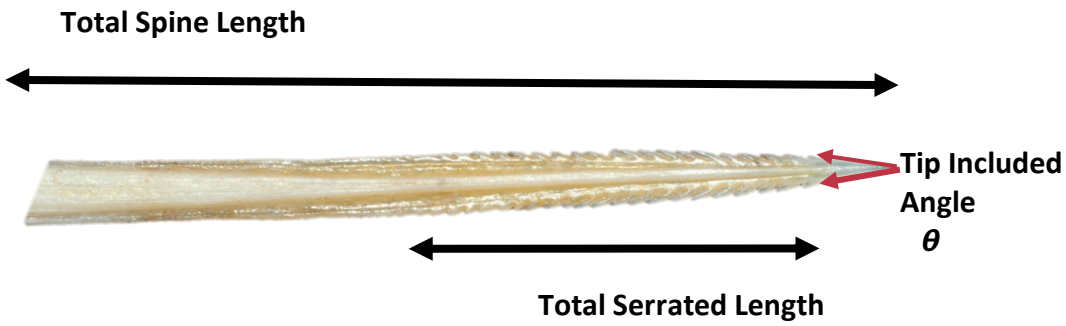

Figure 2: Morphometrics of *H. sabinus* spine. The scale was calibrated with the ruler in frame and used to measure the total spine length (cm) from the tip to the base of the spine in ImageJ. Total serrated length (cm), the length of the spine that was serrated, and the number of serrations was also quantified. The tip included angle was measured with the angle tool in ImageJ. The angle was described from the margins of the left and right lateral edges of the spine to the tip.

Figure 3: Example of Radius of Curvature (RoC) measurements. Data were collected on a digital image of the tip and worked up in ImageJ. R (radius of the circle) denotes the dorsal view. R´ (radius of the circle) denotes the ventral view.

Material testing

Puncture experiments were conducted using porcine skin as the tissue target. Porcine skin is often used in biomedical testing as a proxy for human skin and was obtained from Sierra Medical Group (Whittier, CA; Godin & Touitou, 2007). All porcine skin was thawed and then dissected into 2.54cm squares. A rubber dissection tray was cut into 10x6cm blocks. Small wells (10x10mm, 15mm depth) were cut into the rubber and filled with 5% agar. Above the agar well, the skin was pinned onto the rubber backing with dissection pins (Figure 4). The agar well allowed the spine to pierce through the skin without the added complication of also having to pierce through the rubber backing.

Spines (n=28, n=14 per species) were secured with tension clamps to an Instron E1000 Materials Testing System (Norwood, MA) outfitted with a 250N load cell. The spines were clamped at 50% of total spine length and oriented with the tip facing directly downward into the porcine skin at a 90° angle. Spines were driven into the skin to 20% of the total spine length to standardize the process across different sized spines and to ensure that multiple serrations penetrated the skin (Figure 5). After being embedded, the spine was held in place for 1s prior to starting withdrawal. The spine was withdrawn until the tip was no longer embedded into the target material. Both puncture and withdrawal were at a rate of 30 mm min^{-1} based on previous puncture testing of a barbed spine (Crofts & Anderson, 2018). Each spine was tested only once and a new sample of skin was used for each spine puncture trial.

Micro-CT Scanning

After testing, spines (n=22, n= 11 per species) were wrapped in gauze and packed into a clear canister for micro computed tomography (micro CT) scanning in a Bruker

Skyscan 1173 (Kontich, Belgium). Phantom targets of known mineralization density were scanned simultaneously and were used to calibrate the Skyscan CT-analyzer software (CT-An; Kontich, Belgium). Bone mineralization density (BMD), the volumetric density of calcium hydroxyapatite (CaHA, $g.cm^{-3}$), was calculated at four regions of interest along the length of the spine: tip, 20%, 50% and 90% (base) of the total length of the spine using Bruker DataViewer and CT-An (Kontich, Belgium; Figure 6).

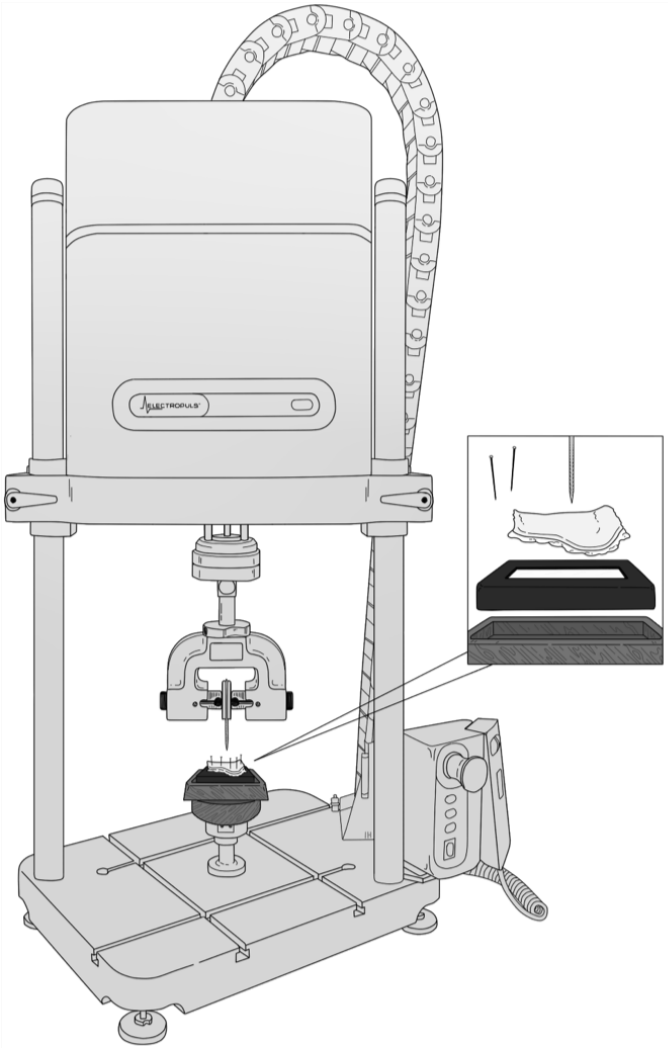

Figure 4: Puncture testing setup on Instron E1000. Spines were held by tension clamps at a 90° angle. Magnified image shows porcine skin sample held in place by pins on top of rubber block with an agar well. Illustration credit: I. Heerdgeen

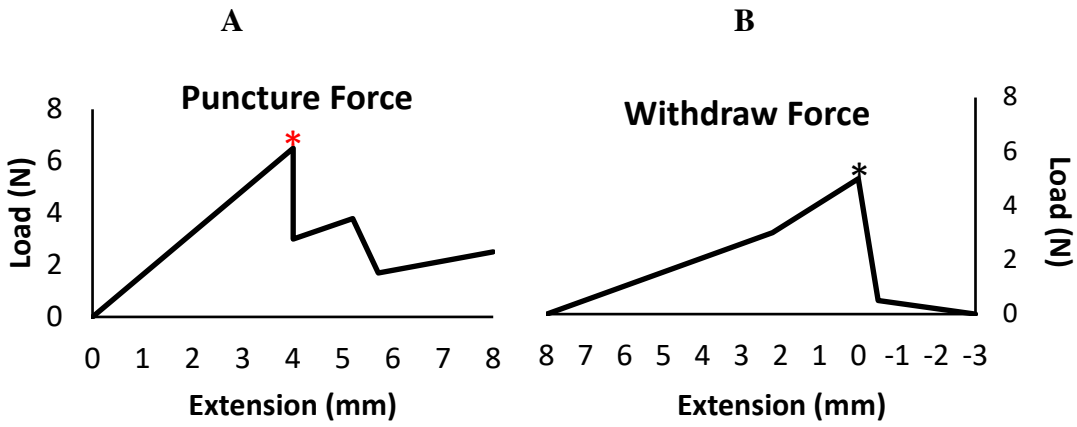

Figure 5: An example of a Puncture and Withdraw on Load/Extension Curve. In this example, tests were set to an extension of 8mm and return back to baseline. A) Puncture force. 10% load drop is indicated by *. B) Withdraw force. * denotes the point at which the spine has exited skin.

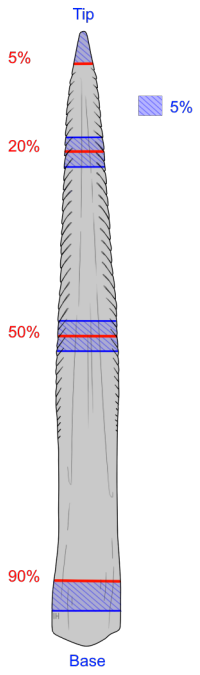

Figure 6: Caudal spine Bone mineralization density (BMD). BMD was determined from interpolated regions of interest in 5% sections along the tip, 20%, 50% and 90% (base) of the total length of the spine. Illustration credit: I. Heerdgeen

Analysis

Data were tested for normality and all statistics were run on R studio. To describe spine morphological characteristics between the two species, I used t-tests and Wilcoxon rank sum tests (Aim i). I expected that both species would have the same spine morphology since they have similar ecologies. I also used linear regressions to investigate the relationships between the total length of the spine and the number of serrations, included tip angle and RoC both pooled and by species (Aim i). Overall, I expected that as spine length increased, the number of serrations would increase. I also expected that the spine length would not correlate with tip sharpness (included tip angle or RoC).

To quantify puncture and withdraw forces and the impacts of spine morphology on those forces, I used a generalized linear mixed model with interaction terms taking into account individuality since some specimens had more than one spine (Aim ii). I expected that withdrawal from the target material would require more force than the puncture, due to the presence, and rear-facing direction, of the serrations. I expected that the serrations would act as stress concentrators, facilitating the cutting of tissue and reducing the force required to penetrate, as seen in barbed cacti spines and porcupine quills (Crofts & Anderson, 2018; Cho *et al*., 2012). I expected that sharper and acute tip included angle spines would require less force to puncture than blunt, more obtuse spines.

To evaluate mineralization among spine regions, I used a Kruskal Wallis rank sum test and a Mann-Whitney Wilcoxon test with Bonferroni corrections (Aim iii). I expected that mineralization would be similar throughout the spine. I also expected that the primary spines would be more mineralized than secondary spines, due to age.

RESULTS

Morphology

One spine (*H. say*) was considered an outlier due to its small size and was not included in any statistical analyses (n=27, n=13 *H. say*, n=14 *H. sabinus*). The caudal spines of the two species did not differ significantly in total length (p=0.2649, T = -1.1405, df=25), serration density (p=0.5377, T = -0.62489, df=25) or RoC (p=0.4929, T = -0.69594, df=25). However, *H. say* spines had a significantly longer serrated portion of the spine compared to *H. sabinus* spines (p=0.024, w=44). The proportion serrated in *H. say* was 61% of total spine length, whereas in *H. sabinus* it was 60%. Overall, *H. say* spines had a significantly greater number of total serrations (mean = 61) compared to *H. sabinus* spines (mean = 45.5, p=0.001038, w=23). Included tip angle also differed among the species. *Hypanus sabinus* tips formed a more acute angle (mean = 16.10 degrees) than *H. say* tips (mean = 19.36 degrees, p=0.00103, T = -3.7133, df=25).

Linear regressions were also run to investigate the relationships between the total length of the spine and the number of serrations, included tip angle and RoC both pooled and by species. There were no significant trends relating total length of the spine to the number of serrations, the included tip angle nor the RoC when the species were pooled. However, two significant relationships were noted when separated by species. For *H. sabinus*, the number of serrations increased with spine length (R^2=0.3129, p=0.03755,

Figure 7). For *H.say*, the included tip angle increased with spine length (R^2=0.4855, 0.008131, Figure 8).

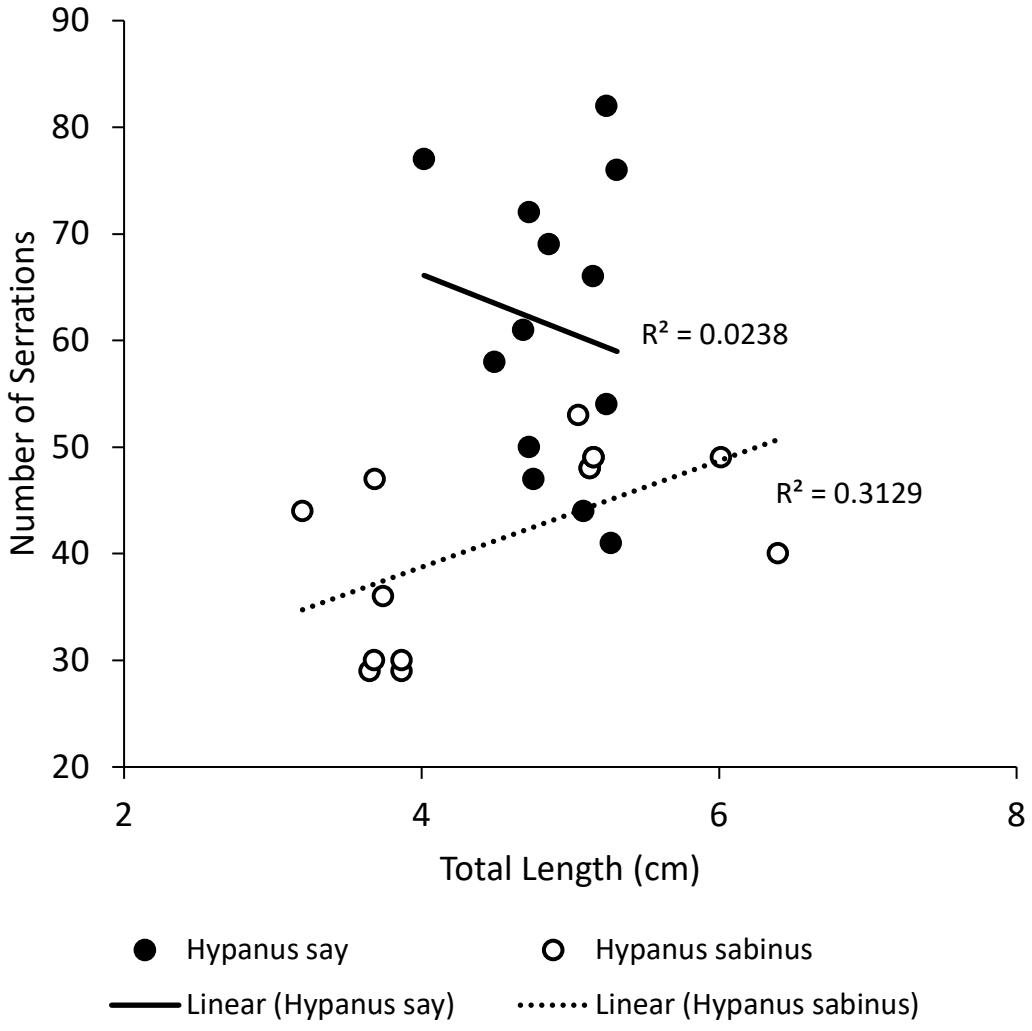

Figure 7: Number of serrations plotted against spine length. As total length (cm) of *H. sabinus* spines increases, the number of serrations also increases (n=14, p= 0.03755). There was no significant relationship between the number of serrations and total length (cm) for *H. say* spines (n=13; p=0.6148).

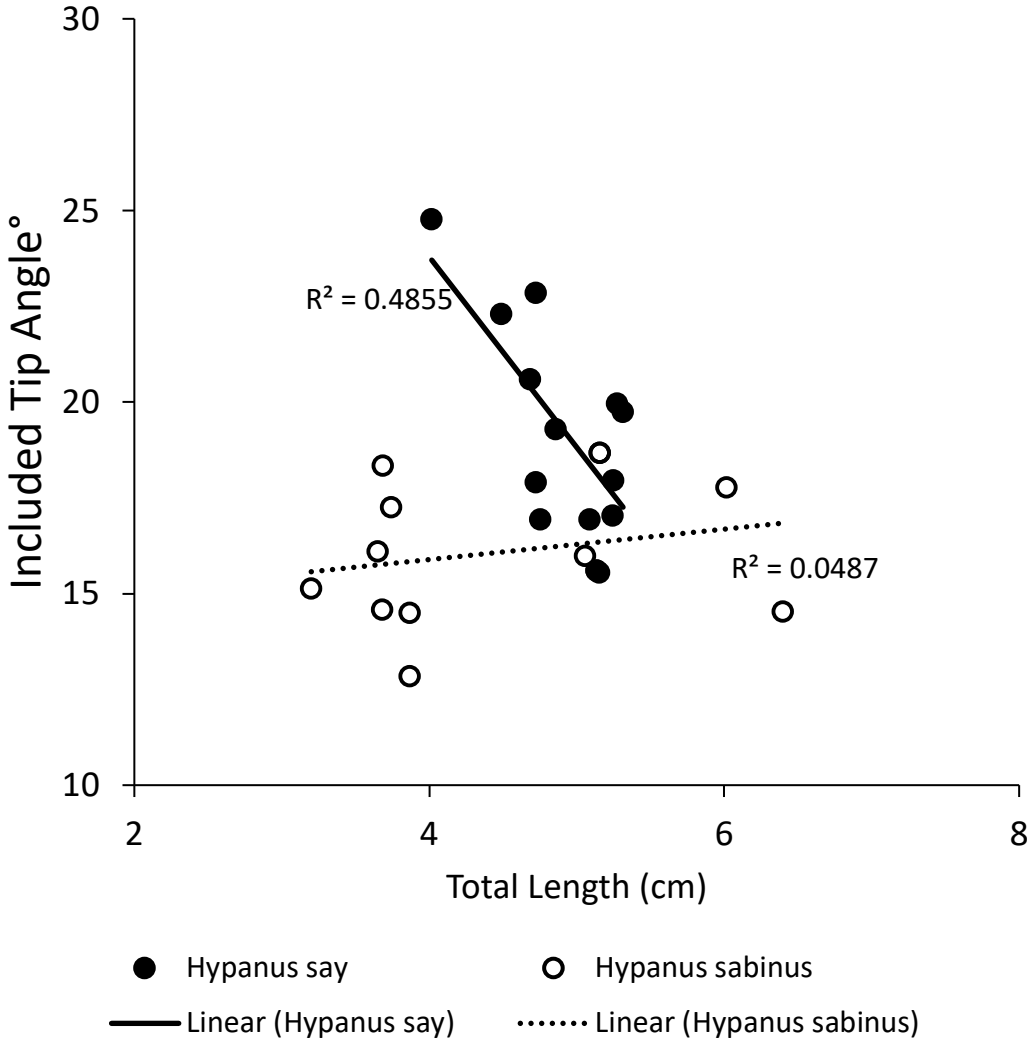

Figure 8: Included tip angle plotted against spine length. As total length (cm) of *H. say* spines increases, included tip angle decreases (n=13; p=0.0008131). There was no significant relationship between included tip angle and total length (cm) for *H. sabinus* spines (n=14; p=0.4481).

Material Testing

To quantify puncture and withdraw forces and the impacts of morphology on those forces, I used a generalized linear mixed model with interaction terms taking into account individuality. There were no significant interactions nor was there a significant difference between puncture and withdraw force (Table 1).

Table 1: Results from Generalized Linear Mixed Model with interaction terms. Interactions between coefficients are noted by *. There were no significant interactions between the test type (puncture and withdraw) and any of the morphological characteristics measured in this study.

Coefficients	**t value**	**p value**	**Coefficients**	**t value**	**p value**
Total Length	0.424	0.674	Total Length* Test Type	0.928	0.359
Test type	0.442	0.661	Serrated Length * Test Type	-0.332	0.742
Serrated Length	0.011	0.991	Serrations along one side* Test Type	0.235	0.816
Serrations along one side	0.276	0.784	Included Tip Angle* Test Type	0.026	0.979
Included Tip Angle	0.382	0.704	RoC* Test Type	-0.709	0.483
RoC	2 0.884	0.383	Serration Density* Test Type	-0.125	0.901
Serration Density	0.229	0.820	Species* Test Type	-0.572	0.571
Species	0.115	0.909	Serrations in total* Test Type	-0.014	0.989
Serrations in total	-0.719	0.477			

Mineralization

To evaluate mineralization among spine regions (species were pooled), I used a Kruskal Wallis rank sum test and a Mann-Whitney Wilcoxon test with Bonferroni corrections. I found that mineralization differed along the length of the spine (Chi-squared = 13.637, df = 3, p = 0.003443). The spine mineralization at the tip was not significantly different from the base of the spine (p=0.129). The spine mineralization in the 20% region was not significantly different from the 50% region along the length of the spine. (p=0.196). However, there was a significant difference between the shaft of the spine (20% and 50%) and the extremities (tip and base) of the spine (p=0.024, p=0.046).

The shaft region of the spine was more mineralized (Table 2). A bimodal distribution of BMD in each region along the spine was noted (Figure 9).

Table 2: BMD value medians for each spine region. The spine is most mineralized along the shaft (p=0.024, p=0.046).

BMD Region	**BMD value medians**
BMD Tip	1.074
BMD 20	1.1455
BMD 50	1.1613
BMD Base	0.9625

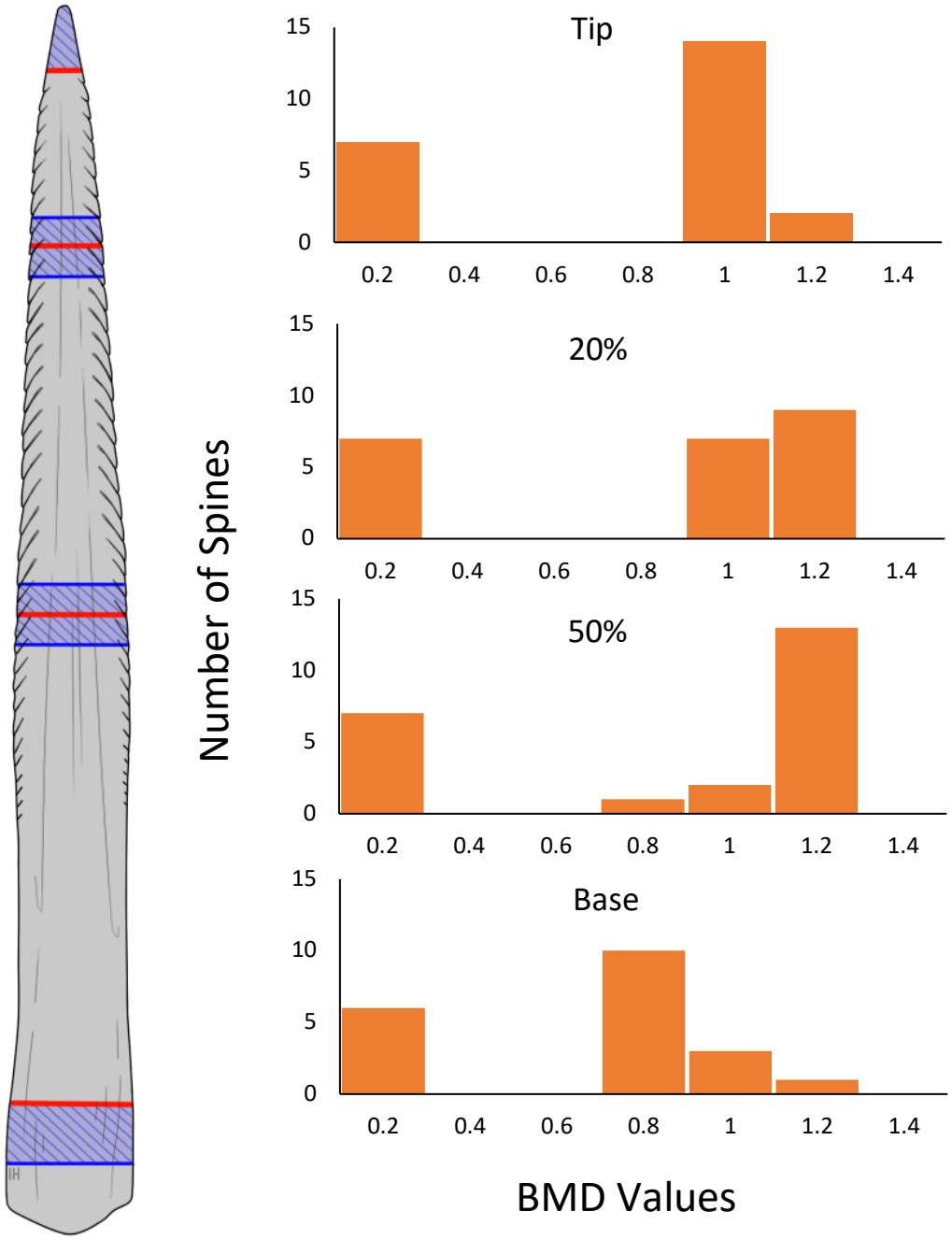

Figure 9: Bimodal distributions of Bone Mineralization Density (BMD) values (n=22). BMD was determined from interpolated regions of interest in 5% sections along the tip, 20%, 50% and 90% (base) of the total length of the spine using Skyscan CT-analyzer.

DISCUSSION

The purpose of this study was to assess caudal spine morphology impacts on the puncture performance of caudal spines from the Bluntnose stingray, *Hypanus say,* and Atlantic stingray, *Hypanus sabinus,* two closely related species *(Genus Hypanus)*. Both stingray species studied occur in shallow, inshore coastal and estuarine habitats (Bigelow & Schroeder, 1953; Thorson, 1983; Snelson *et al*., 1988). Although the two stingray species share similar ecologies, the range distribution of *H. sabinus* is more constrained. *Hypanus sabinus* is distributed from the Chesapeake Bay, USA, to Campeche, Mexico with some freshwater populations (Robins & Ray, 1986). In contrast, *H. say* has a patchy distribution in western Atlantic coastal waters from Massachusetts to southern Brazil, including the Gulf of Mexico and many islands in the Greater Antilles (Bigelow & Schroeder, 1953; Snelson *et al*., 1989). *Hypanus say* is a slightly larger species (50-60 cm) than *H. sabinus* (22-27 cm), but they share a similar diet of small snails, worms and bivalves (Smith, 1997; Dulvy & Reynolds, 1997; Bigelow & Schroeder, 1953; Michael, 1993). Both species are ovoviviparous; gestation period of *H. say* is 10-11 months including a period of embryonic diapause, whereas gestation for *H. sabinus* is 4 months (Last *et al*., 2016). Their overlapping ranges, similar ecologies, and close phylogenetic relationship, would lead us to expect that their spine morphology would be similar.

Morphology

Stingray caudal spines are partially serrated, and I expected that the number of serrations would increase with spine length. Since there was increasing surface area as the spine length increased, I thought that there would be a potential for more serrations since there would be more physical space. I determined that the number of serrations along a spine increased significantly with spine length for only one species, *H. sabinus* (R^2=0.3129, p=0.03755, Figure 7). *Hypanus say* spines have a significantly longer serrated portion of the spine compared to *H. sabinus* spines (p=0.024, w=44). Overall, *H. say* spines had more serrations along their length compared to *H. sabinus* spines (p=0.001332; w=24.5). If *H. say* had a greater number of serrations, but length of the spine did not differ, you would expect that the serration density would differ, but that was not significant. I expected similar spine morphologies because these species are phylogenetically and ecologically similar. However, spine morphology cannot be conclusively linked to ecology nor phylogeny (Chabain, 2020, personal communication). Spine shape can be highly variable in terms of number of serrations, serrated length of spine, and spine cross-sectional shape both inter and intra-specifically (Chabain *et al.,* 2019).

I also hypothesized that the spine length would not correlate with the tip included angle. Included tip angle is a measurement of sharpness; I predicted that length would have no impact on sharpness. Contrary to what I hypothesized, the included tip angle increases as the total length of *H. say* spines increases (R^3=0.4855, 0.008131, Figure 8). It is reasonable that as the spine length increases, that the girth of the spine would also increase. Included tip angle also differed among the species; *H. sabinus* tips were more

acute (and therefore sharper) than *H. say* tips (p=0.00103, T = -3.7133, df=25). Again, these differences may be due to the high variability of this defense structure.

Material Testing

To quantify puncture and withdraw forces and the impacts of spine morphology on those forces, I used a generalized linear mixed model with interaction terms taking into account individuality since some specimens had more than one spine (Aim ii). Organisms puncture for a particular purpose, and those objectives will influence both the morphology of the tool and the behavior during puncture (Anderson, 2018). Defensive biological projections often have surface ornamentation that helps the tool to remain lodged in the target (Haydak, 1951; Schill *et al.,* 1973; Robinson, 1974; Schlegel, 2009, Zhao *et al.,* 2015; Anderson, 2018). I expected that withdrawal from the target material would require more force than the puncture, due to the presence, and rear-facing direction, of the serrations. I expected that the serrations would act as stress concentrators, facilitating the cutting of tissue and reducing the force required to penetrate, as seen in barbed cacti spines and porcupine quills (Crofts & Anderson, 2018; Cho *et al.,* 2012). I expected that sharper and acute included tip angle spines would require less force to puncture than blunt, more obtuse spines.

There were no significant interactions, nor was there a significant difference between puncture and withdraw force for the spines of either species (Table 1). This may be due to characteristics of the spine morphology. Caudal spines are dorso-ventrally compressed compared to the cylindrical shape of cacti spines and porcupine quills (Crofts & Anderson, 2018; Cho *et al.*, 2012). Caudal spine serrations are macroscopic structures, whereas the barbs of cactus spines and porcupine quills are microscopic structures and

cover a greater surface area (Crofts & Anderson, 2018; Cho *et al*., 2012). The barbs on cacti spines and porcupine quills also splay away from the shaft of the biological projection when pulled in the opposing direction (Crofts & Anderson, 2018; Cho *et al*., 2012). During the puncture and withdrawal trials, stingray spine serrations did embed into the skin but did not behave in the same manner as the barbs on cacti spines and porcupine quills (Supplementary Figure 1). Unlike these other spines, the rigid spines of the stingrays did not increase their diameter when being pulled out and the serrations were tightly angled against the spine shaft itself so there was minimal catching of the serration tips on the punctured tissue. Since the stingray spines are rigid and do not change shape from puncture to withdrawal, the width of the puncture wound is the same as that required to withdraw the spine. In contrast, the deployable barbs of the cacti and porcupine effectively increase the size of the biological projection as it is withdrawn. These differences in shape and size could impact serrations performance during the puncture and withdraw trials.

My study mimicked a *vertical* strike as described by Hughes et al. (2018). However, stingrays also utilize a *horizontal* strike, which was not investigated during this study. Perhaps the main purpose of the *vertical* strike is to deliver the venom and for the stingray to escape without major tissue damage. Since the width of the stingray puncture wound is the same as that required to withdraw the spine, it may be that the ultimate goal of the *vertical* strike is venom delivery, since serrations do not impact the withdraw force. In contrast, the serrations may play a more important role during a *horizontal* strike. During a *horizontal* strike, the serrations create lacerations (physical damage) and

seemingly are effective for defense for that reason. This has not been investigated to my knowledge.

Differences in the anatomy of the stingray tail may also contribute to the overall puncturing mechanics. Previous work examined the puncturing mechanics of the yellow stingray, a species with the spine located near the distal tip of a thick, muscular tail. This contrasts to the thin, whip-like tail of my two study species in which the caudal spine is located approximately midway along the length of the tail. These differences in morphology could produce different strike forces. In addition, it remains unexplored whether the whip tail stingrays also exhibit horizontal and vertical strikes, or even if they exhibit a novel form of strike. Differences in strike kinematics and morphology remain to be tested by comparison among species that possess different morphologies.

Mineralization

I expected that mineralization would be similar throughout the spine, but mineralization was not uniform along the spine length. The shaft of the spine (20% and 50%) was significantly more mineralized than the tip ($p=0.024$) and base of the spine ($p=0.046$) (Table 2). Greater mineralization confers greater stiffness, and a stiff material is more brittle and may break easier (Vogel, 2003). If these spines are most brittle in the middle of the shaft then the spine could snap off after it was impaled into a predator. This could allow the stingray to swim away after inflicting damage to a predator and minimize the risk of tissue damage to its own body. A brittle spine tip would likely break prior to penetration and provide only minimal tissue damage to the predator. Similarly, a brittle base would likely cause the spine to break prior to effectively puncturing the spine into its predator.

I also noted a bimodal distribution of BMD in each region along the spine (Figure 9). I had expected that the older primary spines would be more mineralized than the more newly formed secondary spines. The sample size of secondary spines was too small to include in analyses, but the BMD values of the secondary spines fell in the low node of the distributions. It is important to note that spines were only classified as *primary* or *secondary* when two spines were present on an individual. It is possible that some of the spines classified as *primary* (on individuals with only one caudal spine) could be secondary spines, and the *primary* spine had shed or fallen off the animal recently prior to being caught. To test whether BMD is greater in primary spines, it is necessary to sample a greater number of animals that possess two caudal spines. An appropriate sampling time would be from May to August, when *H. sabinus* is known to have two spines prior to shedding the primary caudal spine (Teaf & Lewis, 1987; Amesbury & Snelson, 1997).

CONCLUSION AND FUTURE DIRECTIONS

There are fewer than 164 venomous elasmobranch species (Halstead 1970; Smith & Wheeler, 2006). Of the venomous elasmobranchs (sharks, skates and rays), a few are sharks in the Orders Squaliformes (Family Squalidae) and Heterodontiformes, (Family Heterodontidae) but over 90% are rays from five families (Dasyatidae, Gymnuridae, Myliobatidae, Plesiobatidae, Potamotrygonidae) within the Order Myliobatiformes (Smith & Wheeler, 2006). Every year thousands of people worldwide are stuck by stingray spines (O'Neil *et al*., 2007; Diaz, 2008). This is the result of someone accidentally stepping on a stingray rather than the ray actively seeking out people to puncture in defense of their space. As humans increasingly use nearshore marine environments, stingray-human encounters will likely increase (Lowe *et al*., 2007). By investigating stingray caudal spine puncture performance, I am able to gain a better understanding of this defensive tool, and possibly develop effective mitigation strategies.

I did not find that any of the morphological characteristics measured in my study impacted puncture and withdraw forces, however other morphometrics may have an impact. Serration angle, for example, was not investigated in this study, but the angle of the serrations may play a role in the interaction between puncture and withdraw. Smaller serration angles would potentially not impact puncture and withdraw forces since the serrations would be closer to the shaft of the spine. I expect that the behavior of spines with small serration angles would have similar puncture and withdraw forces. If the spine

had large serration angles, there is a potential for those serrations to have an impact on puncture and withdraw forces since they effectively would increase the size of the biological projection as it is withdrawn. Serration density could also have impacted puncture and withdraw forces. A spine with low serration density could potentially require an increased withdraw force because of the tissue getting caught in the spaces between the serrations. A spine with high serration density would have less space between each serration and therefore it would be less likely that the tissue fibers would catch on the serrations. It is important to note that this study compared the spines from two ecologically and phylogenetically similar species. Despite the reasonably large sample size from each species, I did note a high degree of variation in the spine morphometrics which might have served to obscure some differences between the species. To further investigate the role of morphometrics on puncture and withdraw forces, it would be valuable to compare spines from more ecologically and phylogenetically diverse taxa, such as Urolophidae and Urotrygonidae stingrays (round stingrays) since they have a muscular tail. It would also be good to investigate freshwater stingrays and other Myliobatid stingrays with different ecologies, since the study species in this research were very similar ecologically and phylogenetically.

This study used porcine skin as a model for human skin, primarily to investigate the impacts of tissue damage to humans. However, the stingray spine evolved as a defensive mechanism against predators, so it would be valuable and informative to test the puncture mechanics in different target materials, such as shark buccal cavity skin. In all puncture events, the target sustains tissue damage but the magnitude of the puncture wound may differ dramatically based on the material properties of the target tissue.

Future work could elucidate the efficacy of the stingray spine on its intended tissue target.

In the future, spine tips should be photographed under higher magnification to facilitate more accurate measurements of the radius of curvature. In this study, the spines were photographed prior to puncture, to eliminate any tip damage that might occur during puncture. As a result, the spines were not able to be imaged using a scanning electron microscope because the intact spines were too big to fit within the imaging chamber. A higher magnification image would provide a better description of the tip of the spine for analysis. In addition, RoC radii should be taken from the dorsal and lateral perspectives to quantify sharpness, rather than dorsal and ventral which merely replicate each other.

While not all of our findings supported our hypotheses, I do note that morphology can impact tool punctures and withdraw mechanics. To my knowledge, this is the first study to quantify the forces required to puncture and withdraw stingray spines. Therefore, there exist numerous opportunities for future studies to build upon this work.

APPENDIX

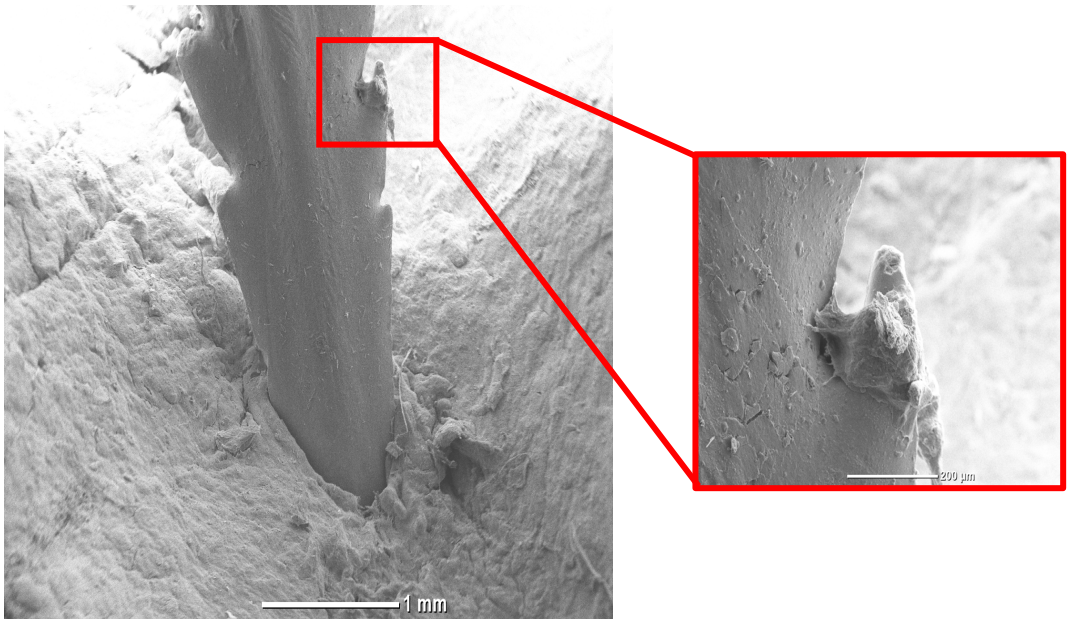

Supplementary Figure 1: Scanning electron microscope image example of *H. sabinus* caudal spine tip embedded in 5mm thick porcine skin during puncture trials. Inset shows porcine skin tissue that remains on serrations after withdrawal.

REFERENCES

Allen, T.B. (1999). *The Shark Almanac*. The Lyons Press, New York.

Anderson, P.S.L., LaCosse J., & Pankow, M. (2016). Point of impact: the effect of size and speed on puncture mechanics. *Interface Focus.* (6):20150111.

Anderson, P.S.L. (2018). Making a point: shared mechanics underlying the diversity of biological puncture. *J Exp Biol.*. (221):1-12.

Amesbury, E., & Snelson Jr., F.F. (1997). Spine replacement in a freshwater population of Atlantic stingray, *Dasyatis sabina*. *Copeia*. (1):220–223.

Auerbach, P. (1991). Marine envenomations. *N Engl J Med.*. (325):486–493

Betz, O., & Kölsch, G. (2004). The role of adhesion in prey capture and predator defense in arthropods. *Arthropod Struct Dev.* (33):3-30.

Bigelow, H.B., & Schroeder, W.C. (1953). *Fishes of the western North Atlantic. Part 2. Sawfishes, guitarfishes, skates, rays, and chimaeroids*. Memoirs Sears Foundation for Marine Research, Yale University, New Haven, Connecticut.

Bone mineral density (BMD) calibration in Skyscan CT-analyser. Method note. 1-8. Bruker Corporation. Belgium.

Chabain, J.J., Summers, A.P., & Kolmann, M.A. (2019, January 4-6). What's the point?: form and function of the caudal barb in stingrays (Talk). Society for Integrative and Comparative 2019 Annual Meeting, Tampa, FL.

Cho, W.K, Ankrum, J. A., Guo, D., Chester, S.A., Yang, S.Y., Kashyap, A., Campbell, G.A., Wood, R.J., Rijal, R. K., Karnik, R., Langer, R., & Karp, J.M. (2012) Barbs enhance tissue penetration and adhesion. *PNAS.* 109 (52): 21289-21294.

Cliff, G., & Dudley, S.F.J. (1991). Sharks caught in the protective gill nets of Natal, South Africa. 4: The Bull shark *Carcharhinus leucas* Valenciennes. *Afr J Mar Sci.* (10):253-270.

Crofts, S.B., & Anderson, P.S.L. (2018). The influence of cactus spine surface structure on puncture performance and anchoring ability is tuned for ecology. *Proc. R. Soc. B* (285):20182280.

Crofts, S.B., Lai, Y., Hu, Y., & Anderson, P.S.L. (2019). How do morphological sharpness measures relate to puncture performance in viperid snake fangs? *Biol Lett.* (15)4:20180905.

DeVries, M.S., Murphy, E.A.K., & Patek, S.N. (2012). Strike mechanics of an ambush predator: the spearing mantis shrimp. *J Exp Biol. (*215): 4374-4384.

Diaz, J. (2008) The evaluation, management, and prevention of stingray injuries in travelers. *J Travel Med.* 15(2):102–109.

Duignan, P.J., Hunter, J.E.B., Visser, I.N., Jones, G.W., & Nutman, A. (2000). Stingray Spines: A Potential Cause of Killer Whale Mortality in New Zealand. *Aquat Mamm.* (26)2: 143–147.

Dulvy, N.K. & Reynolds, J.D. (1997). Evolutionary transitions among egg-laying, live-bearing and maternal inputs in sharks and rays. *Proc R Soc Lond Ser B: Biol Sci.* (264):1309-1315.

Enzor, L.A., Wilborn, R.E., & Bennett, W.A. Toxicity and metabolic costs of the Atlantic stingray (*Dasyatis sabina*) venom delivery system in relation to its role in life history. *J Exp Mar Biol Ecol.* (409):235-239.

Fenner, P., Williamson, J., & Burnett, J. (1996) Clinical aspects of envenomation by marine animals. *Toxicon.* 34(2):145.

Galloway, K.A., & Porter, M.E. (2019) Mechanical properties of the venomous spines of *Pterois volitans* and morphology among lionfish species. *J Exp Biol.* (222): jeb197905.

Godin, B., & Touitou, E. (2007). Transdermal skin delivery: predictions for humans from in vivo, ex vivo and animal models. *Adv Drug Deliv Rev.* (59):1152-1161.

Gudger, E.W. (1914). History of the spotted eagle ray, *Aetobatis narinari*, together with a study of its external structures. *Carnegie Institute Washington*. (183): 248–323.

Gudger, E.W. (1946). Does the stingray strike and poison fishes? *Sci. Mon.,* 63 (2),110-116.

Halstead, B.W., & Bunker, N. (1953). Stingray attacks and their treatment. *Am J Trop Med Hyg*. (2):115–128.

Halstead, B.W., Ocampo, R.R., & Modglin, F.R. (1955). A study on the comparative anatomy of the venom apparatus of certain North American stingrays. *J Morphol*. 97 (1) 1-21.

Halstead, B.W. (1970). *Poisonous and venomous marine animals of the world. Vol. 3* U.S. Government Printing Office, Washington, D.C.

Haydak, M. H. (1951). How long does a bee live after losing its sting? *Glean. Bee Cult.* 79, 85-86.

Hughes, R., Pedersen, K., & Huskey, S. (2018). The kinematics of envenomation by the yellow stingray, *Urobatis jamaicensis*. *Zoomorph*.137(3), 409–418.

Huskey, S.H. (2017). *The skeleton revealed: an illustrated tour of the vertebrates*. Johns Hopkins University Press, Baltimore.

ImageJ, National Institute of Health, Open source image processing software, Bethesda Maryland, v. FIJI (2018).

Johansson, P.K.E., Douglass, T.G., & Lowe, C.G. (2004). Caudal spine replacement and histogenesis in the round stingray, *Urobatis halleri*. *Bull South Cali Acad Sci* 103(3):115-124.

Last, P.R., White, W.T., de Carvalho, M.R., Séret, B., Stehmann, M.F.W., & Naylor, G.J.P. (2016). *Rays of the world.* CSIRO Publishing, Comstock Publishing Associates.

Le Sueur, C.A. (1817). Description of three new species of the genus *Raja*. *J Acad Nat Sci Phila*. 1(3): 41–45.

Lesueur, C.A. (1824). Description of several species of the Linnaean genus *Raia*, of North America. *J Acad Nat Sci Phila*. 4 (1): 100–121.

Lowe, CG., Wetherbee, B.M, Crow, G.L, & Tester, A.L. (1996) Ontogenetic dietary shifts and feeding behavior of the tiger shark, *Galeocerdo cuvier,* in Hawaiian waters. *Enviro Bio of Fishes. (*47): 203-211.

Lowe, C.G., Moss, G.J., Hoisington, G.I.V., Vaudo, J.J., Cartamil, D.P., Marcotte, M.M., & Papastamatiou, Y.P. (2007). Caudal spine shedding periodicity and site fidelity of round stingrays, *Urobatis halleri* (Cooper), at Seal Beach, California:

Implications for stingray-related injury management. *Bull South Calif Acad Sci* (106):16–26.

National Marine Fisheries Service (NMFS). (2006) Status report on the continental United States distinct population segment of the goliath grouper (*Epinephelus itajara*).

Marmi, J., Vila, B., Oms, O., Galobart A., & Cappetta, H. (2010) Oldest records of stingray spines (Chondrichthyes, Myliobatiformes), *J Vertebr Paleontol.* (30)3: 970-974.

Michael, S.W. (1993). *Reef sharks and rays of the world: A guide to their identification, behavior, and ecology*. Sea Challengers, Monterey, California.

O'Neil, M.E., Mack, K.A., & Gilchrist, J. (2007). Epidemiology of non-canine bite and sting injuries treated in U.S. emergency departments, 2001–2004. *Public Health Report.* 122(6):764–775.

Perkins, R., & Morgan, S. (2004). Poisoning, envenomation, and trauma from marine creatures. *Am Fam Physician*. (69):885–890.

Randall, J.E. (1967). Food habits of reef fishes of the West Indies. *Stud Trop Oceanogr.* (5): 665-847.

Russell, F.E. (1965). Marine toxins and venomous and poisonous marine animals. *Adv. Mar. Biol.* (3): 255-384.

Robins, C.R., & Ray, G.C. (1986). *A field guide to Atlantic coast fishes*. Houghton Mifflin, Boston, MA.

Robinson, H. (1974). Scanning electron microscope studies of the spines and glochids of the Opuntioideae (Cactaceae). *Am. J. Bot*. (61): 278-283.

Salisbury, S.M., Martin, G.G., William, M.K., & Schulz, J.R. (2010) Venom kinematics during prey capture in *Conus*: the biomechanics of a rapid injection system. *J Exp Biol*. (213):673–682

Schill, R., Barthlott, W., & Ehler, N. (1973). Mikromorphologie der Cactaceen-Dornen. *Trop. Subtrop. Pflanzenwelt* (6): 262-279.

Schlegel, U. (2009). The composite structure of cactus spines. *Bradleya* (27): 129-138.

Schneider, C.A.; Rasband, W.S., & Eliceiri, K.W. (2012). NIH Image to ImageJ: 25 years of image analysis. *Nat Methods* 9(7): 671-675.

Schwimmer, D.R., Stewart, J.D., & Williams, G.D. (1997). Scavenging by sharks of the genus Squalicorax in the Late Cretaceous of North America. *Paleo.* (12): 71-83.

Schwartz, F. (2005). Tail spine characteristics of stingrays (Order Myliobatiformes) found in the northeast Atlantic, Mediterranean, and Black Seas. *Electron J Ichthyol.* (1):1-9.

Schwartz, F. (2007). A survey of tail spine characteristics of stingrays frequenting African, Arabian to Chagos-Maldive Archipelago waters. *Smithiana Bulletin.* (8): 41-52.

Shimada, K. (1997). Paleoecological relationships of the Late Creataceous lamniform shark, *Creatoxyrhina mantelli* (Agassiz). *J Paleontol*. (71)5: 926-933.

Snelson Jr., F.F., Mulligan, T.J., & Williams, S.E. (1984). Food habitats, occurrence, and population structure of the bull shark, *Carcharhinus leucas*, in Florida coastal lagoons. *Bull. Mar. Sci.* (34): 1:71-80.

Snelson Jr., F.F., Williams-Hooper, S.E., & Schmid, T.H, (1988). Reproduction and ecology of the Atlantic Stingray, *Dasyatis sabina*, in Florida coastal lagoons. *Copeia.* (3):729-739.

Snelson Jr., F.F., Williams-Hooper, S.E., & Schmid, T.H. (1989). Biology of the Bluntnose Stingray, *Dasyatis sayi*, in Florida coastal lagoons. *Bull Mar Sci.* 45:1. 15-25.

Smith, C.L. (1997). *National Audubon Society field guide to tropical marine fishes of the Caribbean, the Gulf of Mexico, Florida, the Bahamas, and Bermuda*. Alfred A. Knopf, Inc., New York.

Smith, W.L., & Wheeler, W.C. (2006). Venom evolution widespread in fishes: a phylogenetic road map for the bioprospecting of piscine venoms. *J Hered*. (97)3: 206-217.

Spieler, R.E., Fahy, D.P., Sherman, R.L., Sulikowski,J., & Quinn, T.P. (2013) The yellow stingray, *Urobatis jamaicensis* (Chondrichthyes Urotrygonidae): a synoptic review. *Carib J Sci*. 47(1):67–97.

Stevens, J.D., & Lyle, J.M. (1989). Biology of three Hammerhead sharks (*Eusphyra blochii, Sphyrna mokarran and S. lewini*) from Northern Australia. *Aus J Mar Fresh Res*. (40):129-146.

Su, X., Kamat, S., & Heuer, A.H. (2000). The structure of sea urchin spines, large biogenic single crystals of calcite. *J Mater Sci.* (35): 5545.

Su, F.Y., Bushong, E.A., Deerinck, T.J., Seo, K., Herrera, S., Graeve, O.A., Kisailus, D., Lubarda, V.A., & McKittrick, J. (2017). Spines of the porcupine fish: Structure, composition, and mechanical properties. *J Mech Behav Biomed.* (73):38–49.

Teaf, C. M., & Lewis, T.C. (1987) Seasonal Occurrence of Multiple Caudal Spines in the Atlantic Stingray, *Dasyatis sabina* (Pisces: Dasyatidae). *Copeia*. (1):224-227.

Thorson, T. B. (1983). Observations on the morphology, ecology, and life history of the euryhaline stingray, *Dasyatis guttata* (Bloch and Schneider) 1801. *Acta Biol Venez*. (11):95-125.

Vogel, S. (2003). *Comparative Biomechanics: Life's Physical World*. Princeton: Princeton University Press.

Zhao, Z.L., Zhao, H.P., Ma, G.J., Wu, C.W., Yang, K., & Feng, X.Q. (2015). Structures, properties, and functions of the stings of honey bees and paper wasps: a comparative study. *Biol Open* (4): 921-928.